

## MECHANICAL DYNAMICS ANALYSIS OF PM GENERATOR USING H-ADAPTIVE REFINEMENT

AJAY KUMAR<sup>1\*</sup>, SANJAY MARWAHA<sup>2</sup>, ANUPAMA MARWAHA<sup>3</sup>

<sup>1</sup>Deptt. of Electronics and Communication Engg, Beant College of Engg. and Tech.,  
Gurdaspur (Punjab), India.

<sup>2</sup>Deptt. of Electrical and Inst. Engg, Sant Longowal Institute of Engg and Tech.,  
Longowal (Punjab), India.

<sup>3</sup>Deptt. of Electronics and Communication Engg, Sant Longowal Institute of Engg  
and Tech., Longowal (Punjab), India.

\*Corresponding Author: ajaykm\_20@yahoo.co.in

### Abstract

This paper describes the dynamic analysis of permanent magnet (PM) rotor generator using COMSOL Multiphysics, a Finite Element Analysis (FEA) based package and Simulink, a system simulation program. Model of PM rotor generator is developed for its mechanical dynamics and computational of torque resulting from magnetic force. For the model the mesh is constructed using first order Lagrange quadratic elements and h-adaptive refinement technique based upon bank bisection is used for improving accuracy of the model. Effect of rotor moment of inertia (MI) on the winding resistance and winding inductance has been studied by using Simulink. It is shown that the system MI has a significant effect on optimal winding resistance and inductance to achieve steady state operation in shortest period of time.

Keywords: Bank bisection, Finite-element analysis, h-adaptivity, Moment of inertia, PM rotor generator.

### 1. Introduction

Permanent magnet (PM) generators have the advantages of eliminating the exciter field winding, slip rings and brushes. The ability of the permanent generator to self-excite is an attractive feature that makes it a suitable choice for operation at higher power factors and efficiencies. PM machines do have the overloading capability and full torque capability at zero and at very low speeds. The understanding

### Nomenclatures

$E$	Estimated error
$G$	Gradient in finite element mesh
$J$	Moment of inertia, $\text{kg/m}^2$
$L$	Length of the model, m
$M$	External torque, Nm
$T$	Electromagnetic torque, Nm
$t$	Time, s

#### Greek Symbols

$\alpha$	Rotation angle, degrees
$\delta$	Specified error tolerance
$\eta_s$	Global error indicator
$\rho$	Density of material, $\text{kg/m}^3$
$\omega$	Angular frequency, rad/s

of the characteristics and accurate modeling of the dynamic performance of these are of fundamental importance to design engineers, as also is the study of power system stability and reliability [1]. Finite element analysis has been used extensively for the design and performance prediction of various types of permanent magnet machines. Usually it complements analytical techniques which can provide a rapid and reliable means of design optimization by using adaptation procedures. Adaptive methods try to distribute the degrees of freedom (DOF) of the problem in such a way that an accurate solution can be obtained maintaining a low number of unknowns [2]. Until recently, the electromagnetic analysis has usually been confined to static representations of the machine geometry using, for example, frequency response methods in synchronous machines [3] or slip frequency analysis in induction motors [4]. This inevitably leads to some inaccuracy in the characterization of the machine. A simulation with independent dynamic electromagnetic and power system analysis [5] is too expensive computationally for everyday design use. Simulations of PM wind turbine generators have been tested for stability [6] are silent about the effect of winding parameters on the steady state performance of the generator.

This paper outlines improvements to the characterization of machine that can be obtained by using dynamic non-linear electromagnetic time-stepping analysis including rotation [7]. Using the 2D software package based upon FEA, model of PM rotor generator is developed for obtaining its mechanical dynamics analysis at the start and subsequent computation of torque. The symmetry of the generator has been exploited to reduce the model size to 1/8th of the original size. For the finite element mesh first order Lagrange quadratic elements has been used. h-adaptive refinement technique based upon bank bisection is used for refining the mesh of the model for improving accuracy. The Simulink Parameter Identification software is then used for optimal parameters analysis.

## 2. System Description

### 2.1. General model

The centre of rotor consists of annealed medium carbon steel, which is a material with high relative permeability. The centre is surrounded with several blocks of permanent magnet made of samarium cobalt, creating a strong magnetic field. The stator is made up of same permeable material as the centre of the rotor. The winding is wound around the stator poles. The winding used in the stator is single turn winding. Length of the generator is 0.4 m. Area of winding in the stator is 0.001257 m<sup>2</sup>. Relative permeability in permanent magnets is 1. To exploit symmetry the smallest possible pole model of the generator is obtained by cutting radially through two adjacent poles as shown in Fig. 1.

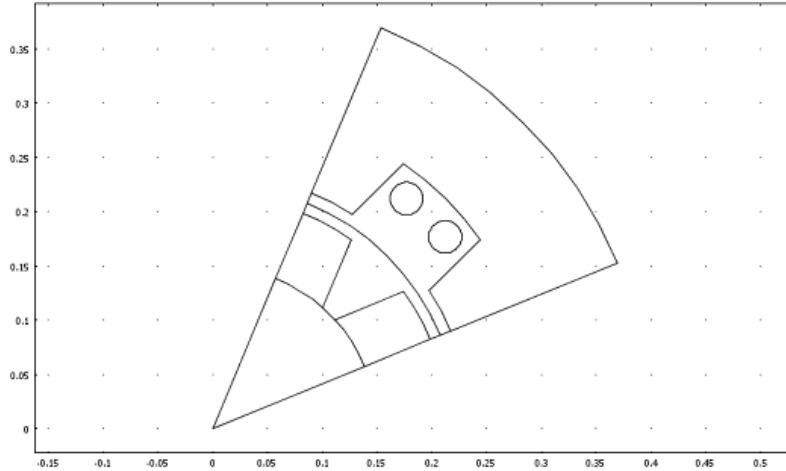


Fig. 1. Model of the Generator.

### 2.2. Theory

The ordinary differential equation for mechanical dynamics [8] is

$$\frac{d^2\alpha}{dt^2} = \frac{T_z + M}{J + J_{rotor}} \quad (1)$$

where  $\alpha$  is the variable rotation angle,  $T_z$  is the electromagnetic torque and  $M$  is the externally applied driving torque.

The electromagnetic torque in the model is computed by boundary integration of the cross product between radius vector  $(x, y)$  and the normal Maxwell stress component  $(nT_x, nT_y)$  over the rotor boundary times the model depth  $L$ .

$$T_z = \int_C 8\rho L(nT_yx + nT_xy)dl \quad (2)$$

The factor 8 is introduced to account for the entire generator.  $J$  is the external MI (flywheel and turbine) and  $J_{rotor}$  is the MI of the rotor. The model computes  $J_{rotor}$  by sub-domain integration of the material density times radius vector squared

times the model depth. Once again, the factor 8 in Eq. (3) is introduced to account for the entire generator.

$$J_{rotor} = \iint_A 8\rho L(x^2 + y^2) dA \quad (3)$$

where  $\rho$  is the material density.

To account for rotation, central part of the geometry containing the rotor and part of air gap is coupled with a rotation transform to the coordinate system of the stator. The vector potential is coupled to a boundary between stator and rotor with the transform [1]

$$\begin{bmatrix} \cos(\omega t) & -\sin(\omega t) \\ \sin(\omega t) & \cos(\omega t) \end{bmatrix} \begin{bmatrix} x_{rotor} \\ y_{rotor} \end{bmatrix} = \begin{bmatrix} x_{stator} \\ y_{stator} \end{bmatrix} \quad (4)$$

The boundary condition is then used to force the vector potential along the boundary in the air gap to the rotated potential.

### 3. Mesh Refinement

#### 3.1. h-adaptive procedure

The flow diagram of h-adaptive mesh refinement procedure is shown in Fig. 2.

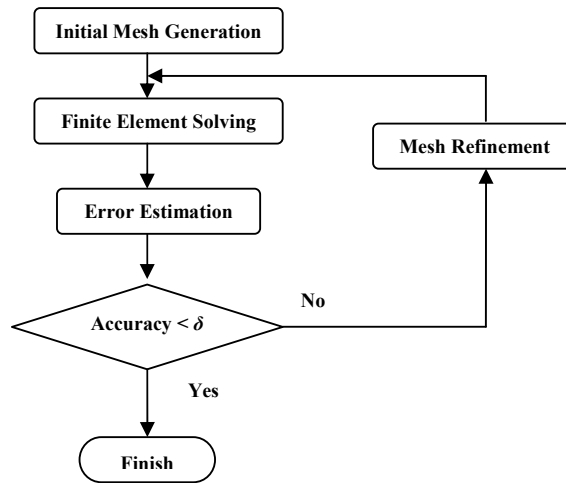


Fig. 2. h-adaptive Mesh Refinement Flow Diagram.

In adaptive analysis, the error estimation provides information about accuracy of the finite element solution as well as an indicator for further mesh refinement. The need of the recovery solution is a necessity of a Posteriori error estimate to adapt the mesh in order to get a more accurate solution. The estimated error in domain  $\Omega$  is given by [2]

$$E_{total} = \int_{\Omega} \|G^{fem} - G^{spr}\|_2 d\Omega \quad (5)$$

where  $G^{fem}$  is the gradient evaluated by the finite element method and  $G^{spr}$  is the so-called recovered or smoothed gradient, which is to be determined. The global indicator of error  $\eta_s$  is given by

$$\eta_s = \frac{E_{total}}{\|G^{spr}\|_2} \quad (6)$$

For adaptive analysis, the relative error of the final solution should satisfy the inequality

$$\eta_s \leq \delta \quad (7)$$

where  $\delta$  is the specified tolerance.

### 3.2. Element split

In an h-refinement approach, commonly used approaches for refining the mesh are longest edge bisection and bank bisection. In longest edge bisection an element is subdivided into two smaller elements by placing a point at the midpoint of longest edge and connecting it to the opposite vertex. The non-conforming meshes are generated by this method and subdivision of elements with hanging nodes is needed [2]. By Bank bisection, shown in Fig. 3, a quadrilateral element is subdivided into four elements by pair wise connecting the mid-points of its opposing sides. By this bisection finally the conforming meshes are obtained [2]. On the next stage during the refinement process only regular elements are refined. It is very important to maintain or improve the regularity of the elements throughout the adaptive procedure because the exactness of the FEM solution is directly related to it. In the present work the refinement approach based upon bank bisection is used.

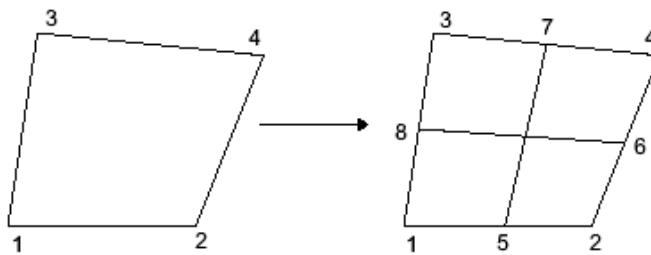
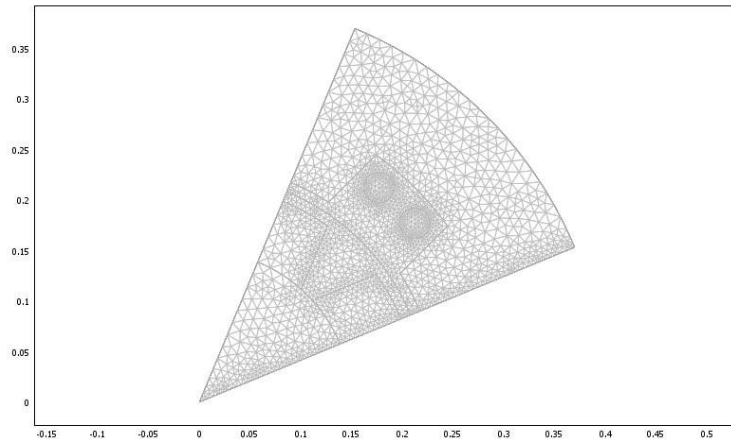


Fig. 3. Bank Bisection Method for the Refinement of Quadrilateral.

## 4. Results and Discussion

The proposed method is applied to a PM generator model of Fig. 4. A finite element mesh, of the model region is constructed using first order Lagrange quadratic elements. The initial mesh, shown in Fig. 5, consists of 3658 elements with 7608 degrees of freedom (DOF). The number of boundary elements in this case is 342. The computed magnetic potential distribution at  $t = 0.2$  s of rotation, by using this initial mesh is shown in Fig. 5. On Intel P4, 3.4 GHz system with

504MB RAM, time taken for this solution was 189.375 seconds. It is apparent from the figure the solution is erroneous at the edges.



**Fig. 4. Initial Mesh in the Generator Consisting of 3658 Elements with 7608 DOF.**

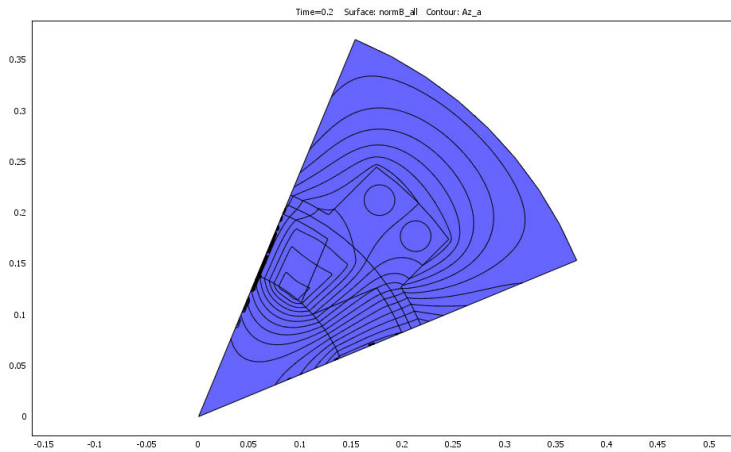


**Fig. 5. Initial Magnetic Potential Distribution without Refinement.**

To improve the accuracy of the solution, the mesh is refined by using bank bisection technique. The refined mesh consists of 14632 elements and 29842 DOF and is shown in Fig. 6. The number of boundary elements in the refined mesh is 684. The magnetic potential distribution using this refined mesh is shown in Fig. 7 for  $t = 2$ s of rotation. Though the solution time in this case is 362.422 seconds, but the solution is free from the error. After assuring the accuracy of the solution, mechanical dynamic analysis of the generator is carried out.

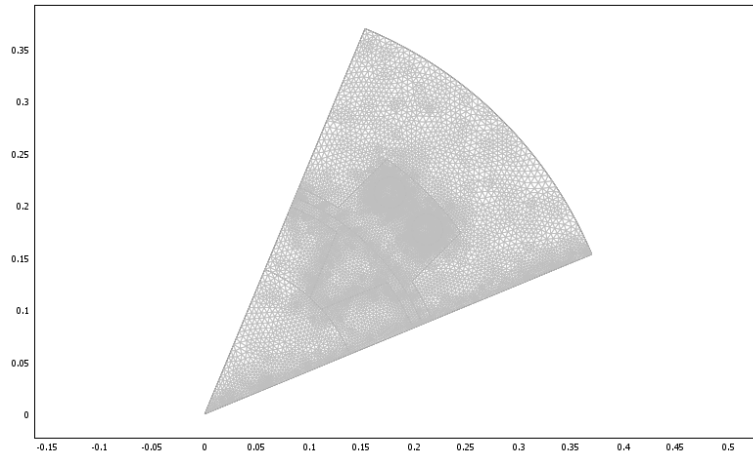


**Fig. 6. Refined Mesh in the Generator Consisting of 14632 Elements with 29842 DOF.**

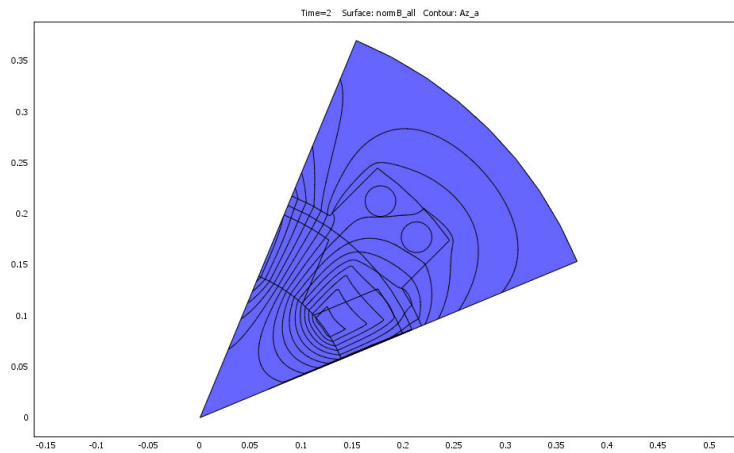


**Fig. 7. Magnetic Potential Distribution in the Generator after 2 s of Rotation.**

The torque curve of the generator during starting is shown in Fig. 8. It is seen that attenuation of transients takes a long time. This is because of larger per unit (pu) inertia of the rotor and winding resistance. Small winding resistance or small inertia helps the generator to pull into steady state easily. The values of the winding resistance, electromotive force and the MI are varied during the simulations. The steady state time is determined from the attenuation of the speed oscillation.

The steady state time as a function of winding resistances and the moment of inertia is shown in Fig. 9. The MI of the system,  $J$ , is compared with the rotor inertia  $J_{rotor}$  of the PM generator. The system MI has a significant effect on the optimum winding resistance value to achieve steady state operation in the shortest

period of time. From Fig. 9, it is seen that when the inertia of the rotating parts is large, the winding resistance has a narrow optimal area. When the inertia of the rotating parts is small, the winding resistances must be selected high enough to guarantee steady state operation.

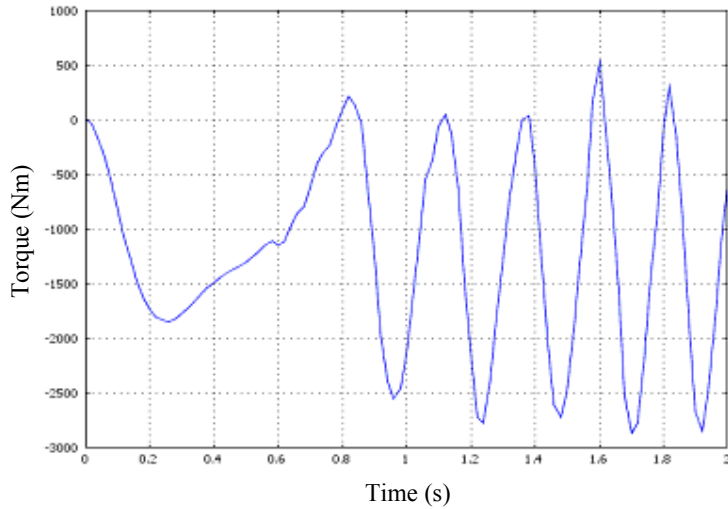


Fig. 8. Torque versus Time Curve.

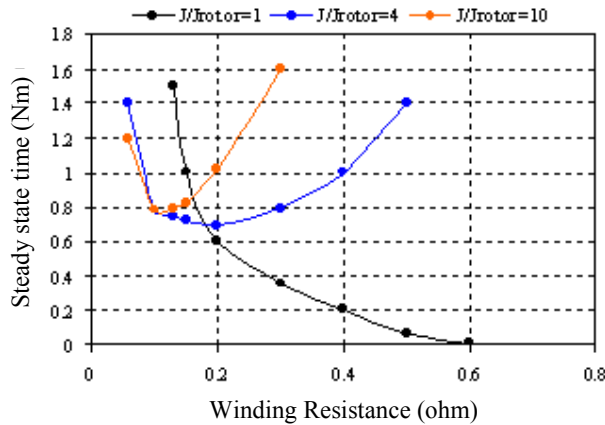
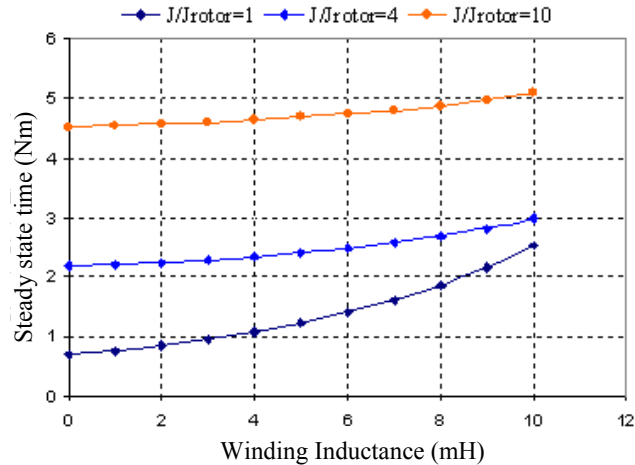


Fig. 9. Steady State Time as a Function of Winding Resistance for Different MI Rotors.

Permanent magnets produce a pulsating magnetic braking torque during the acceleration of the rotor. This braking torque is also responsible for distorting the steady state operation. This braking torque depends upon the winding leakage

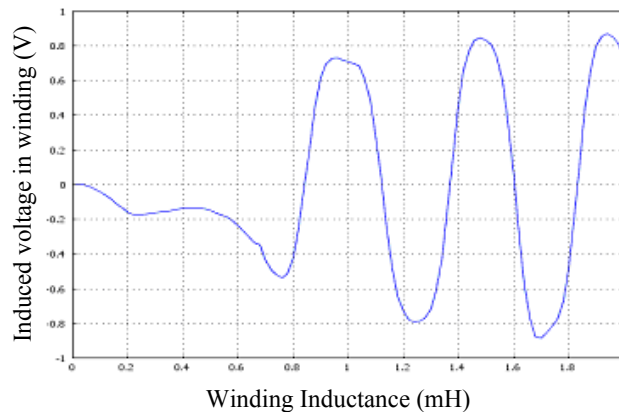


inductance. Again the values of the winding inductance and the MI are varied during the simulations. The steady state time as a function of winding leakage inductance and MI is shown in Fig.10. The system MI,  $J$ , is compared with the rotor inertia  $J_{rotor}$ . From the curve it is concluded that the winding leakage inductance should be reduced for the speedy steady state operation.



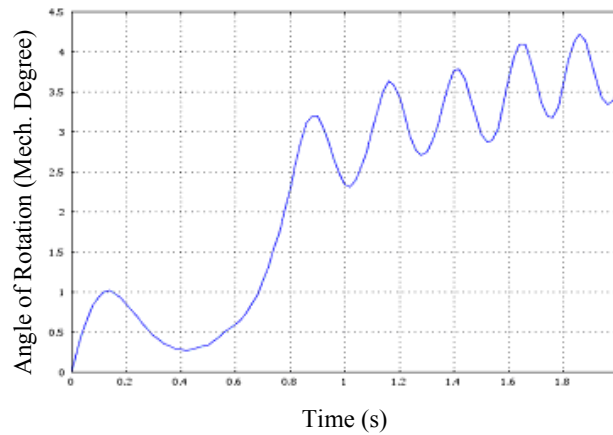
**Fig. 10. Steady State Time as a Function of Winding Inductance for Different MI Rotors.**

Figure 11 shows the voltage induced in the winding. It is seen that voltage starts from zero value and large demagnetizing currents are present during start due to higher MI ratios. Steady state voltage is reached after 0.8 seconds of rotation. The induced current will be of similar shape as the model accounts for the winding current by dividing the induced voltage by winding resistance.



**Fig. 11. Induced Voltage in the Winding.**

Figure 12 shows the rotating angle and hence velocity variation with time during starting. The change at the start is because the generator accelerates more or less because of system MI.



**Fig. 12. Angle of Rotation of Generator.**

## 5. Conclusions

This paper presents the mechanical dynamic analysis of PM magnet generator by using h-adaptive refinement. A 2D package based upon FEM has been used for the study of dynamic behaviour of the generator. The effect of rotor MI and the optimum winding parameters on the steady state operation of the generator has been studied. It is seen that when the inertia of the rotating parts is large, the winding resistance has a narrow optimal area. When the inertia of the rotating parts is small, the winding resistances must be selected high enough to guarantee steady state operation. It has also been shown that by reducing the winding leakage inductance, the braking torque produced by permanent magnets and hence the steady state time of the generator can be reduced.

## Acknowledgement

The authors are highly grateful to the Department of Electrical and Instrumentation Engineering, Sant Longowal Institute of Engineering and Technology, Longowal, Punjab, India, for allowing the use of FEA package of COMSOL Multiphysics 3.2a, for the execution of above work.

## References

1. Kumar, A.; Marwaha, S.; and Marwaha, A. (2008). Finite element 2D modeling of electromagnetic devices taking account of the rotation. *Int J. of Engg. Research and Ind. App.*, 1(3), 95-103.

2. Zhelezina, Elena (2005). *Adaptive finite element method for the numerical simulation of electric, magnetic and acoustic fields*. Ph.D.Thesis, University of Nuremberg-Erlangen, Germany.
3. Dougherty, J.W.; and Minnich, S.H. (1983). Calculation of generator inductances by finite element methods. In: Symposium on synchronous machine modeling for power systems. Studies. *IEEE Power Engineering Society*, Publication 83TH0101-6-PWR.
4. Williamson, S.; Lim, L.H.; and Robinson, M.J. (1990). Finite element models for cage induction motor analysis. *IEEE Trans. Ind. App.*, 26(6), 1007-1017.
5. Emson, C.R.I.; Riley, C.P.; Walsh, D.A.; Ueda, K.; and Kumano, T. (1998). Modeling eddy currents induced by rotating systems. *IEEE Trans. on Magnetics*, 34(5), 2593-2596.
6. Reddy, Sivananda Kumjula (2005). *Operational behavior of a double-fed permanent magnet generator for wind turbines*. M.Sc. Thesis, Massachusetts Institute of Technology, Dept. of Electrical Engineering and Computer Science.
7. Biddlecombe, C.S. ; Simkin, J. ; Jay, A.P. ; Sykulski, J.K. ;and Lepaul, S. (1998). Transient electromagnetic analysis coupled to electric circuits and motion. *IEEE Trans. on Magnetics*, 34(5), 3182-3185.
8. Salon, S.J. (1985). *Finite element analysis of electrical machines*. Kluwer Academic Publishers.